VHF-UHF Monocone Antenna for Ground Penetrating Radar Application

Tamer G. Abouelnaga [1] and Esmat A. Abdallah [2]

[1] Department of Microstrip Circuits
Electronics Research Institute, Giza, Egypt
Higher Institute of Engineering and Technology-Kafr Elsheikh, Egypt
tamer@eri.sci.eg

[2] Department of Microstrip Circuits
Electronics Research Institute, Giza, Egypt
esmataa2@hotmail.com

Abstract ─ This paper introduces a VHF-UHF monocone antenna for ground penetrating radar GPR application. The proposed antenna covers different bandwidths through only changing the cone geometry. Same ground plane shape and feeding system are used. Firstly, both conventional and proposed monocone antennas are designed, simulated and their simulated results are compared. One antenna cone is fabricated and measured for verification purpose. Good agreement is obtained between measured and simulated bandwidths. The measured bandwidth extends from 73 MHz to 500 MHz. Secondly, another antenna cone is designed and simulated without altering the upper or the lower cone radii. The second cone antenna bandwidth extends from 130 MHz to 1000 MHz. The receiver antenna of the commercial SIR 2000 impulse GPR is replaced by the proposed VHF-UHF first monocone antenna and the field test results are recorded and discussed.

Index Terms ─ GPR, MCA.

I. INTRODUCTION

Ground Penetrating Radar uses electromagnetic waves to locate and characterize objects beneath the ground surface. The main components of a typical GPR system are illustrated in Fig. 1. The transmitter generates an electric signal, which is radiated by the transmitting antenna. At receiver, reflections from above and below the ground are gathered, digitized, and stored for processing and interpretation. High and low frequencies are used to detect small size and deep buried objects, respectively. GPR's usually operate in the VHF-UHF electromagnetic spectrum. Frequencies as low as 20 to 50 MHz are used for locating deep caves, mine tunnels, water detection or ice thickness measurement. Frequency of 150 MHz is a typical center frequency for cart mounted radars. Frequencies as high as 300 to 500 MHz are used for shallow and high-resolution probing [1].

The performance of GPR depends on the proper design of transmitter and receiver (T/R) antennas. Many antennas were developed to cover the VHF-frequency band such as microstrip antenna [2, 3], VHF spiral antenna [4], compact multiband VHF antenna [5], monopole cone antenna [6], electrically small broadband printed monopole antenna [7], conformal VHF antenna [8], and conical monopole antenna [9]. Table 1 shows a comparison of the aforementioned antennas.

Table 1: VHF antennas

Reference	Bandwidth (MHz)	Antenna Size (cm^3)
[2-3]	127-172	116 x 116 x 26.66
[4]	90 - 300	295 x 295 x 100
[5]	37.6 - 38.1, 72.9 – 74, 150.4 - 151.9	271,6 x 207.9 x 5
[6]	53.6 - 500	120 x 120 x 150
[7]	165 - 175	39 x 31 x 0.1
[8]	95 - 241	116 x 62
[9]	70 - 220	400 x 400 x 74.4

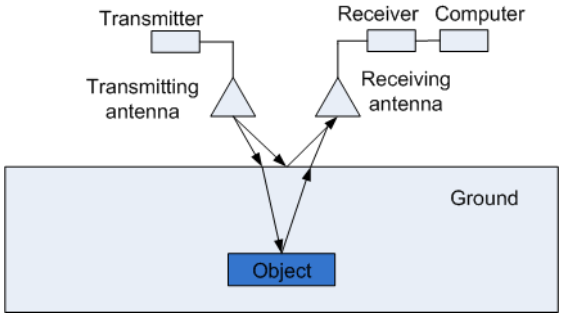

Fig. 1. Illustration of a typical GPR system.

In this paper the proposed antenna is designed to cover different bandwidths of the VHF/UHF frequency bands. The proposed compact VHF-UHF-MCA antenna

Submitted On: March 22, 2016
Accepted On: January 26, 2019

covers the bandwidths from 73 to 500 MHz and from 130 to 1000 MHz when first and second cones are used, respectively. The proposed VHF-UHF-MCA has dimensions of 70 cm by 70 cm by 90 cm. The paper explains antenna design in second section. Measuring and fabrication are introduced in section three. Finally, the conclusions section is presented in section four.

II. ANTENNA DESIGN

In wireless communication systems, conventional wire monopole is one of the most widely used antennas due to its low cost, omni-directional radiation patterns, simple structure, and ease for matching to 50 Ohm [10]. Also, it is unbalanced, thus balun is eliminated, which may have a limited bandwidth [11]. Bandwidth increases with the increase of the radius-to-length ratio, this indicates that a fatter structure will lead to a broader bandwidth because the current area, and hence the radiation resistance is increased [12]. However, when the monopole radius is too large related to the feeding line, the impedance mismatch between them will become significant and the bandwidth can't be further increased.

As stated by Victor Rumsey in the 1950s [13], that the impedance and pattern properties of an antenna will be frequency independent if the antenna shape is specified only in terms of angles. So, a conical shape can be used instead of wire structure. The main challenge in this paper is to design a conical monopole antenna operating in the VHF-UHF frequency bands and has considerable light weight for field measurement purpose.

In Section IIA, a conventional VHF-UHF Monocone antenna is designed and simulated using CST and HFSS for comparison purpose. The proposed compact VHF-UHF-MCA with modified ground plane shape is introduced. Effect of the probe tip load is studied using CST simulator. Also, the performance of the proposed antenna with its second cone is investigated.

A. Conventional VHF-UHF monocone antenna

Figure 2 (a) shows the three-dimensional view of the axially symmetric conventional VHF-monocone antenna. This antenna is designed based on [14]. It consists of a metallic cone with top radius R_t, bottom radius R_b, height h and a circular metallic ground plane with radius R_g. A probe feed method is used as feeding scheme.

The conventional VHF-MCA is simulated using both CST and HFSS simulators, Fig. 2 (b). The difference between the two solvers is related to the different boundary conditions which are used by both CST and HFSS simulators. Both CST and HFSS solvers are based on Finite Element Time Domain numerical methods. CST simulator and HFSS are used to analyze the antenna different structure throughout the whole paper.

The resonance frequency of conventional VHF-UHF-MCA is 70 MHZ and its -10 dB bandwidths extend from 54 MHz to 146 MHz, 197 to 230, 281 to 416 and all the curve points are under -8.4 dB. The antenna occupy a cone volume of $9.16 \times 10^5\ cm^3$ and ground plane area of 6842.67 cm^2 which is a major problem for any moving GPR system.

Stutzman and Kim in [15] and [16] had introduced a stable radiation pattern and a model for the monocone antenna, respectively. When increasing the ground plane size of monocone antenna, the performance will be quite similar to the biconical antenna but with an input impedance of half value of the biconical one. Theoretically, infinite length biconical antenna is capable of providing frequency-independent impedance.

The impedance is given by the following expression:

$$Z_o = 120ln\left(cot\frac{\theta}{2}\right), \quad (1)$$

where θ is the angle of the cone, as shown in Fig. 2 (a), and Z_o is the characteristic impedance of the antenna. In practice, the size is truncated which introduces reflections and limits the operating bandwidth, [17]. So, when the monocone antenna's ground plane radius reach certain value, input impedance performance will not be affected much with more increment. This can be clearly seen in Fig. 2 (c).

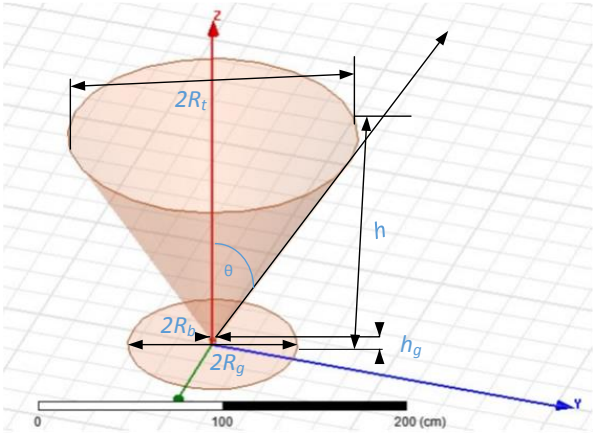

(a)

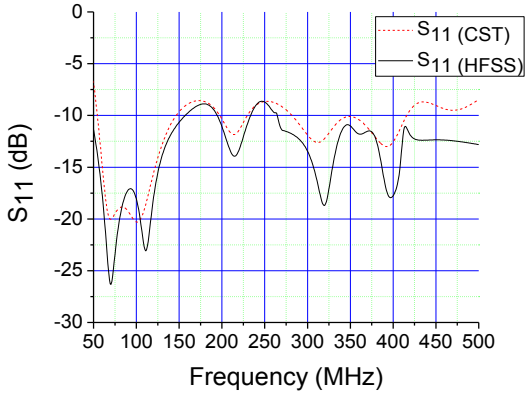

(b)

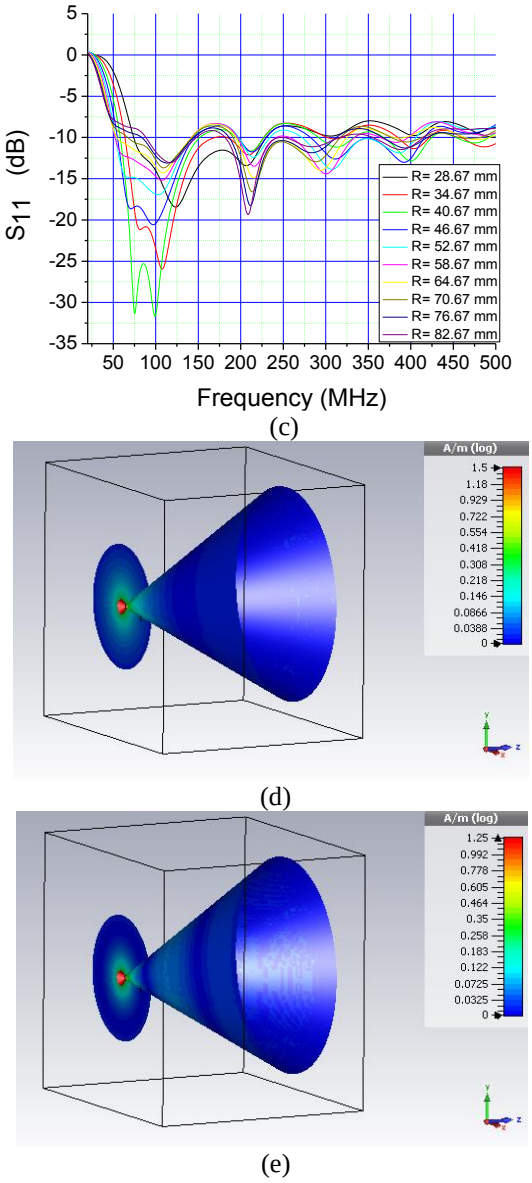

Fig. 2. (a) Conventional VHF-MCA antenna, (b) Conventional VHF-Monocone antenna reflection coefficient versus frequency, (c) Conventional VHF-Monocone antenna reflection coefficient versus frequency at different ground radii, (d) Conventional VHF-Monocone antenna surface current distribution at 100 MHz, and (e) Conventional VHF-Monocone antenna surface current distribution at 215 MHz.

Table 2 shows that, as the ground plane radius increases from 28.67 mm to 46.67 mm, the resonant frequency has shifted back from 123 MHz to 97 MHz, respectively. As ground plane radius increases from 52.67 mm to 58.67 the resonant frequency has shifted forward from 104.5 MHz to 108 MHz, respectively. As the radius increase from 64.67 mm to 82.67 mm, it can be noticed that the resonant frequency is kept at 110 MHz and the antenna reflection coefficient does not change much. So, the size of ground plane doesn't affect much the resonant frequency, but it can be used for matching enhancement process. However, if the ground plane size has been reduced, the antenna may not be frequency dependent anymore.

The surface current distribution of the conventional monocone antenna is shown in Figs. 2 (d) and (e) where the current is concentrated at the cone bottom and at the center area of the ground plane. The proposed antenna will have a bigger ground surface area through using a hollow cube instead of simply a conductor sheet. The center area where the surface current is concentrated is kept as it is. The outer area will be removed and is replaced by an outer ring. By this structure both frequency dependent performance and the surface current distribution may be kept almost the same and the proposed structure will be lighter.

Table 2: CMCA resonance frequency at different ground radii

Resonant Frequency (MHz)	S_{11} **(dB)**	**Ground Plane Radius** R_g **(mm)**
123	-18.5	28.67
107	-26	34.67
99.5	-31.5	40.67
97	-20.6	46.67
104	-17	52.67
108	-15.2	58.67
110	-14.28	64.67
110	-13.7	70.67
110	-13.04	76.67
110	-12.8	82.67

B. Proposed VHF-UHF monocone antenna

The proposed VHF-UHF monocone antenna consist of a metallic cone with radius R_t at the top, R_b at the bottom of the cone and height h. The 3D ground plane is shaped as a hollow metallic box with removed bottom face. This hollow box is welded with a metallic ring with radius R_g. Four steel strips with thickness of 3 mm and width of 4 cm are used to connect the four box sides with the ring, Fig. 3. The feeding scheme consists of probe feed loaded at its probe tip with rectangular metal of 4 cm by 4 cm.

Figure 4 (a) shows the effect of the rectangular metal load on the antenna matching. One can note that as the rectangular load size is increased the better is the matching which add an additional degree of freedom in matching adjustment process. After many trials using CST simulator, the ground plane box is found to be 50 x 50 x 20 cm^3 and the surrounded outer ring radius is 35.5 cm. The resonance frequency of the proposed compact VHF-UHF MCA is 88 MHZ and its -10 dB bandwidths extend from 78.6 MHz to 107 MHz, 176 to 300, 387 to 492, Fig. 4 (b). Figure 4 (c) shows that the proposed

antenna gain is reduced by 0.25 dB at 100 MHz and 2 dB at 350 MHz. the gain reduction is expected because of size reduction. The antenna occupy a cone volume of $1.19 \times 10^5\ cm^3$, ground plane area of 3959.19 cm^2 and weight of 23 kg.

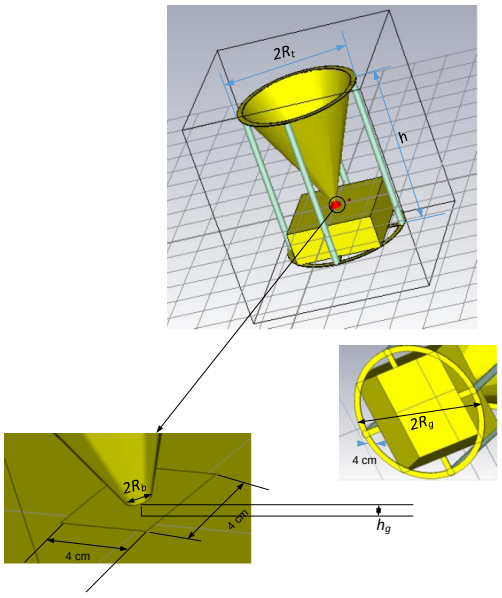

Fig. 3. Compact VHF-MCA antenna.

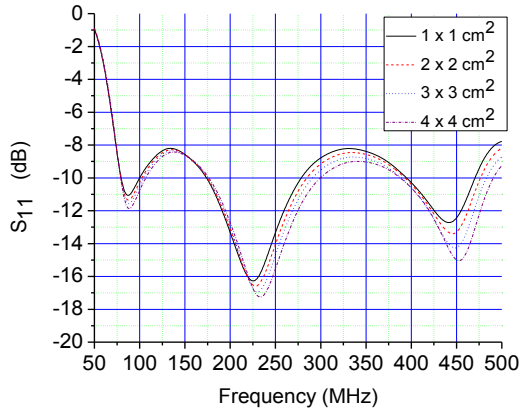

(a)

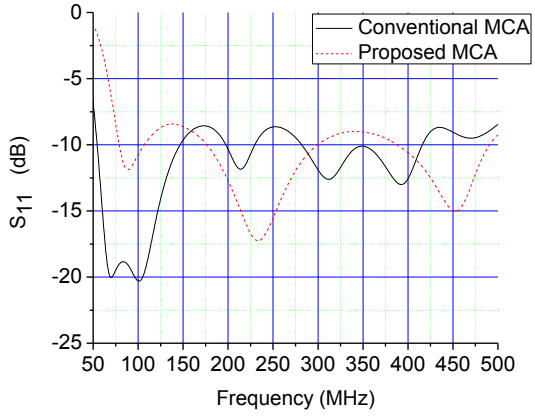

(b)

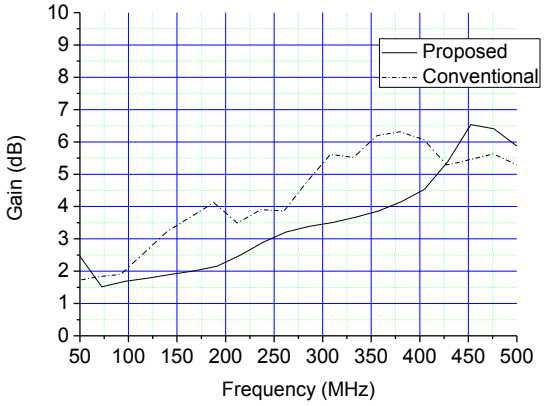

(c)

Fig. 4. (a) Metal rectangular load size effect versus frequency, (b) Conventional MCA and proposed MCA with its first cone reflection coefficients versus frequency, and (c) Conventional VHF-UHF MCA and proposed MCA with its first cone gain versus frequency.

The radiation pattern of the proposed antenna with its first cone is shown in Fig. 5. It can be noticed that the 3-dB beam width becomes narrower as the resonance frequency increases from 230 to 440 MHz, respectively. Same antenna feeding is used and the cone geometry is changed. For mechanical assembling simplicity, only the height of the cone is changed from 90 cm to 60 cm. The cone upper and lower radii are kept at the same values. The simulated bandwidth of the second cone antenna extends from 130 MHz to 1000 MHz, Fig. 6 (a). Also it can be noticed that the 3-dB beam width becomes narrower, Figs. 6 (b) and (c) as the frequency increases from 250 to 800 MHz, respectively.

Table 3 shows a comparison between the dimensions of conventional VHF-MCA, proposed VHF-UHF MCA and SATIMO commercial MCA. It can be noticed that the proposed MCA is much smaller and lighter than SATIMO commercial MCA.

Table 3: Conventional VHF-MCA (CMCA), proposed VHF-UHF MCA and SATIMO MCA

Antenna	**CMCA**	**VHF-MCA**	**SATIMO-MCA**
R_t (cm)	80	35.5	39.75
R_b (cm)	1.667	0.5	5
h (cm)	136.66	90	74.4
R_g (cm)	46.67	35.5	200
h_g (cm)	3.33	1	~1
Weight (Kg)	-	23	159

Table 4 shows a comparison between the radiation parameters of the proposed antenna when first and second cone geometries are used.

Table 4: Proposed VHF-MCA radiation parameters

Antenna	First Cone VHF-UHF MCA		Second Cone VHF-UHF MCA	
Frequency (MHz)	230	440	250	800
Main lobe direction (degree)	60	25	120	15
3 dB beamwidth (degree)	74.7	28.9	115.5	17.5

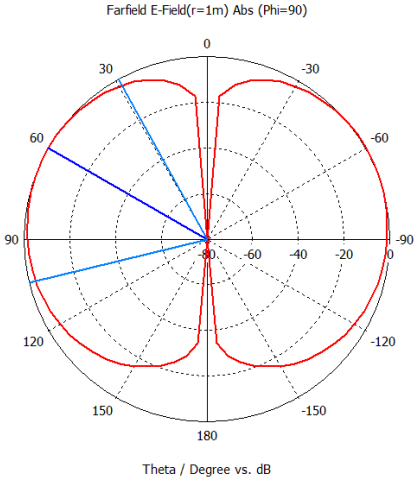

(a)

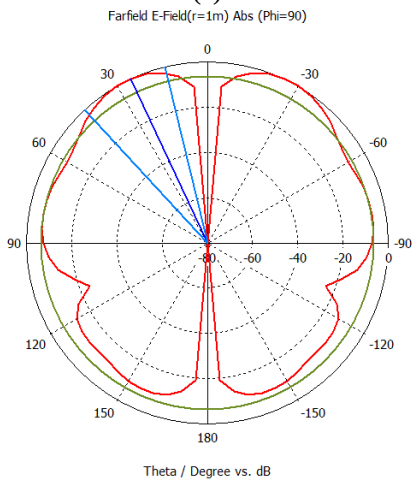

(b)

Fig. 5. (a) Proposed VHF-UHF MCA with its first cone radiation pattern at 230 MHz, and (b) proposed VHF-UHF MCA with its first cone radiation pattern at 440.

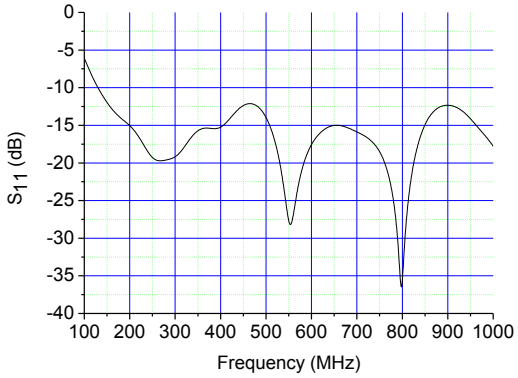

(a)

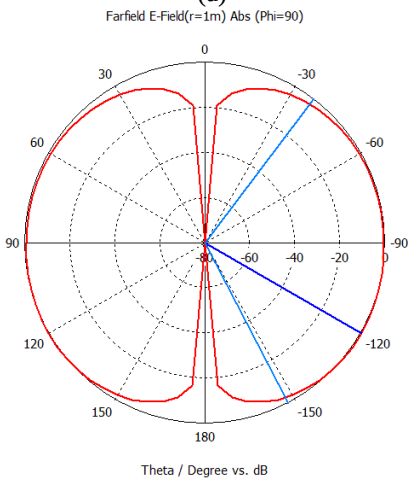

(b)

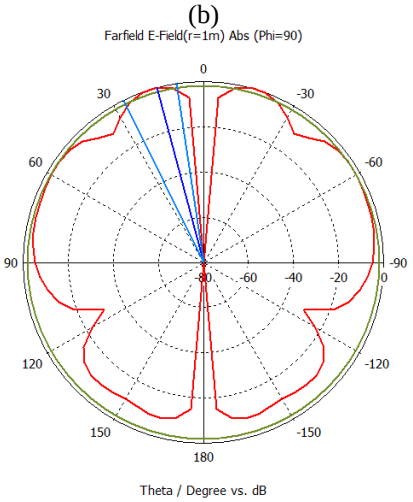

(c)

Fig. 6. (a) Proposed VHF-UHF MCA with its second cone reflection coefficients versus frequency, (b) proposed VHF-UHF MCA with its second cone radiation pattern at 250 MHz, and (c) proposed VHF-UHF MCA with its second cone radiation pattern at 800 MHz.

III. MEASUREMENT AND FABRICATION

A. Proposed VHF-UHF antenna Measurement

The proposed VHF-UHF monocone antenna is fabricated in a high precision workshop. The antenna design is aimed to make the antenna compact, lightweight and mechanically assembled and disassembled, Fig. 7. The proposed ground plane is reshaped as metallic ring which is fasten to a parallel rectangular. Teflon posts are used to connect the metallic ring with cone piece. Eight metallic nails are used to connect cone antenna piece with the ground through the four Teflon posts. The proposed first cone VHF-UHF MCA antenna is simulated and measured. One notices that the simulated -10 dB (SWR = 2) bandwidth is extended from 80.5 MHz to 103 MHz, 171 MHz to 308.5 MHz and from 383 MHz to 500 MHz. The measured frequency bandwidth is better than the simulated one and extends from 73 MHz to 500 MHz, Fig. 8. This discrepancy between measured and simulated results can be referred to that the cone position is not fixed on the tip of the N type connector so, it could be move a little bit from the cone center.

Fig. 7. Practical first cone VHF-MCA photo.

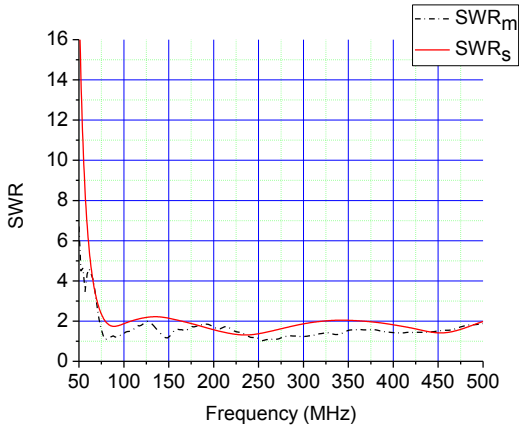

Fig. 8. First cone VHF-UHF MCA simulated and measured SWR versus frequency.

B. Proposed antenna measurement using SIR 2000 GPR system

The GPR system basically consists of transmitter, receiver and controller units. The transmitter unit includes a signal generator, power amplifiers, and transmitter antenna. The receiver unit includes a receiver antenna, a low-noise amplifier (LNA), a sample and hold detector, mixer or demodulator, and analog-to-digital converter (ADC). The controller unit includes a timer, a synchronizer of T/R units, microcontroller, and a data acquisition card. Finally, the raw data are processed to obtain clear subsurface imaging for the detection and identification of buried objects.

The GPR system scan vertically (y axis) and horizontally (x axis), i.e., the y axis presents the depth and x axis present the horizontally distance to be scanned. Designed conical antenna is tested by attaching it to the SIR 2000 GPR model instead of its commercial one at the receiver side. Commercial bowtie antenna of resonance frequency of 100 MHz is used at transmitter side.

The most typical shape found in the obtained GPR images is the hyperbola that corresponds to some targets like pipes and buried objects. These targets appear as hyperbolic shapes because they enter in the emission cone of the antenna in 3 certain space domains surrounding their actual location. The presence of these shapes in the profiles can sustain further calculation of the medium properties. Also, we had placed two metal objects to test how accuracy could our test setup reach.

Figure 9 shows the depth in cm on the vertical axis and the scanned distance in cm on horizontal axis. The horizontal part from 25 cm to 450 cm, shows useful signal with some detected objects at horizontal distance of 450 cm and vertical depth of 100 cm under the earth surface. This results agree well with the obtained results where commercial antenna is installed.

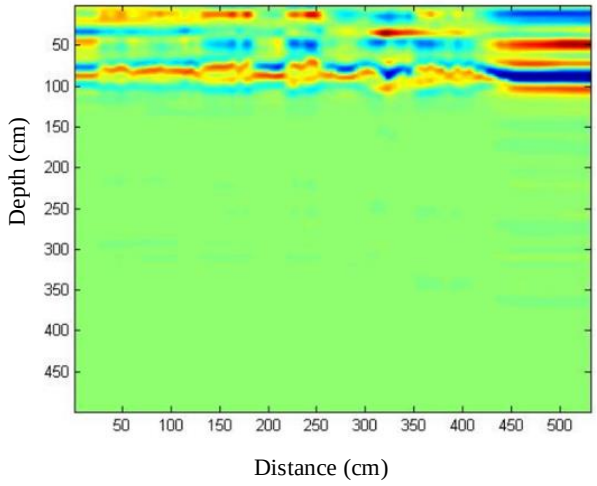

Fig. 9. Scanned image from SIR 2000 GPR system using the proposed VHF-UHF MCA.

IV. CONCLUSIONS

The proposed VHF-UHF MCA antenna was introduced for the GPR application. It was shown that the proposed antenna was easily assembled and disassembled. The antenna covered the bandwidth from 73 MHz to 500 MHz with its first cone. Good agreement was obtained between measured and simulated results. Also the antenna could cover the bandwidth from 130 to 1000 GHz when second cone is used. The antenna was tested using the SIR 2000 GPR model and the results was recorded and investigated.

REFERENCES

[1] R. J. Fontana, "Recent system applications of short-pulse ultra-wide band technology," *IEEE Trans. Microwave Theory Tech*., vol. 52, no. 9, pp. 80-87, Sep. 2004.

[2] J. Huang, Z. Hussein, and A. Petros, "A VHF microstrip antenna with wide-bandwidth and dual-polarization for sea ice thickness measurement," *IEEE Trans. Antennas and Propagat*., vol. 55, no. 10, pp. 2718-2722, Oct. 2007.

[3] A. Petros, J. Huang, and Z. Hussein, "A wide-band dual-polarized VHF microstrip antenna for global sensing of sea ice thickness," in *IEEE Antennas and Propagat. Society International Symposium*, Washington, DC, USA, pp. 684-687, July 3-8, 2005.

[4] R. J. Barton, P. Collins, P. Crittenden, M. Havrilla, and A. Terzuoli, "A compact passive broadband hexagonal spiral antenna array for VHF remote sensing," in *IEEE International Geoscience and Remote Sensing Symposium*, Barcelona, Spain, pp. 593-595, July 23-28, 2007.

[5] R. Anwar, N. Misran, M. Islam, and G. Gopir, "Compact multiband VHF antenna for transient radio telescope," in *International Conference on Space Science and Communication*, Negeri Sembilan, Malaysia, pp. 182-185, Oct. 26-27, 2009.

[6] T. Abouelnaga and E. Abdallah, "Two in one VHF-conical monopole antenna for GPR application," *IEEE Radar Conference*, Cincinnati, OH, USA, pp. 88-92, May 19-23, 2014.

[7] M. R. Abraham and S. O. Kundukulam, "Wide-band printed monopole VHF antenna," in *IEEE International Conference on Computing and Network Communications*, Trivandrum, India, pp. 833-837, Dec. 16-19, 2015.

[8] D. L. Zeppettella and M. Ali, "VHF antenna for airfoil structural integration," in *IEEE International Symposium on Antennas and Propagat. (APSURSI)*, Fajardo, Puerto Rico, pp. 1861-1862, June 26-July 1, 2016.

[9] Antenna catalog, SATIMO-ORBIT/FR, Dec. 2011.

[10] C. Balanis, *Antenna Theory Analysis and Design*. John Wiley and Sons Inc., New Jersey, USA, 2016.

[11] M. J. Ammann and Z. N. Chen, "Wideband monopole antennas for multi-band wireless systems," *IEEE Antennas and Propagat. Magazine*, vol. 45, no. 2, pp. 146-150, Apr. 2003.

[12] A. W. Rudge, K. Milne, A. D. Olver, and P. Knight, *The Handbook of Antenna Design*. Peter Peregrinus Ltd, London, UK, 1982.

[13] V. H. Rumsey, "Frequency-independent antennas," *IRE National Convention Record*, vol. 5, pp. 114-118, 1957.

[14] C. Balanis, *Modern Antenna Handbook*. John Wiley and Sons Inc., New York, USA, 2008.

[15] W. L. Stutzman, *Antenna Theory and Design*. John Wiley and Sons Inc., New York, USA, 1998.

[16] K. H. Kim, J. Kim, and S. O. Park, "An ultrawide-band double discone antenna with the tapered cylindrical wires," *IEEE Trans. on Antennas and Propagat*., vol. 53, no. 10, pp. 3403-3406, Oct. 2005.

[17] D. McNamara, D. Baker, and L. Botha, "Some design considerations for biconical antennas," in *Antennas and Propagat. Society International Symposium*, Boston, USA, pp. 173-176, June 25-29, 1984.

Tamer G. Abouelnaga was born in November 1976, he received his B.Sc. degree in Electronics Engineering from Menofiya University, Egypt, in May 1999, M.Sc. and Ph.D. degrees in Electrical Communication from Ain Shams University in July 2007 and June 2012, respectively. He worksas a Researcher in Microstrip Circuits Department, Electronic Research Institute, Cairo. He had published 30 papers, 19 papers in peer-refereed journals and 11 papers in international conferences in the area of RFID, TEM horn and DRA antennas design. His current research interests are in power dividers, RFID antennas and breast cancer detection. He participates in research projects in the area of GPR and digital beam forming circuits.

Esmat A. Abdallah graduated from the Faculty of Engineering and received the M.Sc. and Ph.D. degrees from Cairo University, Giza, Egypt, in 1968, 1972, and 1975, respectively. She was nominated as Assistant Professor, Associate Professor and Professor in 1975, 1980 and 1985, respectively. In 1989, she was appointed President of the Electronics Research Institute ERI, Cairo, Egypt, a position she held for about ten years. She became the

Head of the Microstrip Department, ERI, from 1999 to 2006. Currently, is at the Microstrip Department, Electronics Research Institute, Cairo, Egypt. She has focused her research on microwave circuit designs, planar antenna systems and nonreciprocal ferrite devices, and recently on EBG structures, UWB components and antenna and RFID systems. She acts as a single author and as a co-author on more than 127 research papers in highly cited international journals and in proceedings.